Analysis and Application of New Quasi-Network Characteristics of Nonuniform Mesh in FDTD Simulation

Yan Zhang, Ben-Qing Gao, *Senior Member, IEEE*, Wu Ren, Zheng-Hui Xue, and Wei-Ming Li

***Abstract*—The equation of computing the reflection coefficient between two meshes of different sizes is derived. Using the equation, quasi-network characteristics of nonuniform mesh for the finite-difference time-domain technique is found and analyzed. The so-called mesh network (MN) here is a kind of structure composed of the sections of mesh in cascade. The cell sizes of these sections change regularly. By means of choosing the number of mesh sections, length of each section, and cell sizes, some novel network characteristics are obtained, which can be used to match the reflecting wave of nonuniform mesh or improve the transmitted characteristics for a mesh wave to travel along the nonuniform mesh. Formulas for analyzing the MN are given. The characteristics are realized in both one- and three-dimensional cases. The applications and advantages of the MN are shown by computing three different structures, i.e., microstrip-gap capacitor, parallel-coupling filter, and microstrip slot-line transformer.**

***Index Terms*—Finite-difference time-domain (FDTD) algorithm, mesh-network (MN) characteristics, mesh wave impedance (MWI), nonuniform mesh.**

I. Introduction

IT IS WELL known that the finite-difference time-domain (FDTD) algorithm is a kind of efficient method of computational electromagnetics. The uniform mesh is usually used in FDTD numerical simulation, but in many cases, the nonuniform mesh techniques are used to save the storage or model the object accurately. The techniques of nonuniform mesh, such as a sub-cell and expanding grid algorithm, etc. [1]–[8], have been proven useful to improve the efficiency and accuracy of the FDTD method. Much attention has been paid to develop and use these techniques, while the effect of nonuniform mesh on computation is often ignored. When a structure of nonuniform mesh is used in the direction of wave propagation, a wave reflection between the meshes of different sizes will occur since their mesh wave impedances (MWIs) are different [9]. Thus, an error is taken into FDTD computation. This paper presents a way to evaluate the effect and make use of it to decrease the error in FDTD analysis, which also gives a reference to choosing the size of the mesh when the nonuniform meshes are used. In addition, the modification of the conventional FDTD algorithm to deal with the sub-gridded region usually requires interpolation or extrapolation in the space and time domain [7]. Using the method of mesh network (MN) in this paper, there will be no need to modify the FDTD program.

When studying the characteristics of the reflecting wave between meshes, we found that the structures composed by regularly arranged nonuniform meshes, which are similar to some networks (i.e., MNs), have corresponding characteristics of those microwave networks, such as a mesh impedance transformer, low-pass filter, and low-pass impedance transformer. When the meshes are arranged in these ways, it is convenient to evaluate the characteristics of nonuniformity of its meshes. In addition, the reflection of the MN can be controlled easily by choosing the section numbers and the length of each, as well as the cell sizes.

In this paper, the formula of reflection between two meshes of different sizes is obtained in terms of MWI. The method for analyzing the MN characteristics is then given in Section II. The characteristic of the MN is realized in Section III. Its applications are then discussed in Section IV.

II. Analysis

A. MWI and Mesh Wave Reflection (MWR)

The wave reflection between two different meshes is considered first. For a plan wave (a one-dimensional (1-D) case) with cell size Δ and time increment Δt, MWI can be written as [9]

$$Z_m = \sqrt{\frac{\mu}{\varepsilon}}\sqrt{\frac{e^{-jk\Delta}-1}{1-e^{jk\Delta}}}e^{-j\omega\Delta t/2}. \tag{1}$$

Set c as the cell-size factor and Δ as the basic cell size, thus, the size of any cell is $c\Delta$. Suppose a wave propagates from a mesh of size $c_1\Delta$ to a mesh of size $c_2\Delta$, the reflection coefficient can be written as follows:

$$R = \frac{Z_{m2}-Z_{m1}}{Z_{m2}+Z_{m1}} = jtg\frac{\phi(c_2)-\phi(c_1)}{2} = jtg\frac{k\Delta(c_2-c_1)}{2} \tag{2}$$

where ϕ is the phase of Z_m. Equations (1) and (2) can be used to quantitatively estimate the reflection between two meshes. The curves in Fig. 1 shows the variation of R with frequency when $c = 0.7, 2, 3, 4$, respectively. The reflection between two meshes increases when the frequency and their cell sizes vary.

Manuscript received May 20, 2001; revised November 28, 2001. This work was supported by the National Natural Science Foundation under Grant 69931030, and by Doctoral Programs in Institutions of Higher Learning, China.

Y. Zhang was with the Electronic Engineering Department, Beijing Institute of Technology, 100081 Beijing, China. She is now with the Shanghai Bell Ltd. Company, 201206 Shanghai, China.

B.-Q. Gao, W. Ren, Z.-H. Xue, and W.-M. Li are with the Electronic Engineering Department, Beijing Institute of Technology, 100081 Beijing, China.

Digital Object Identifier 10.1109/TMTT.2002.804635

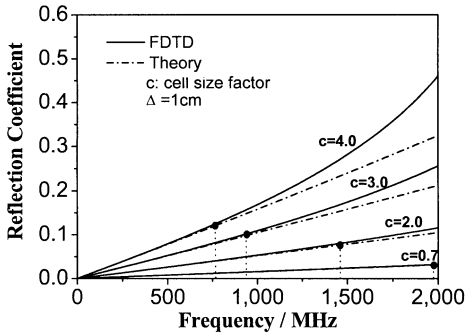

Fig. 1. Reflection coefficient varying with frequency and cell-size factor.

Fig. 1 also gives the results of FDTD computation (dotted line). Two kinds of results are in good agreement when $f < f_c$ (f_c is the criterion frequency marked by (•) in Fig. 1).

From the above analysis, we can see that Z_m and R bear the following characteristics.

1) Both Z_m and R are vectors in the complex plane and functions of frequency.
2) Within the band of criterion frequency, the magnitude of Z_m has no relation with the cell-size Δ and mesh-size factor c.
3) The magnitude of R between two meshes has only a relation with the difference of their cell-size factor c.
4) For a certain time span, the phase of MWI is the function of Δ and c.

Therefore, generally speaking, the sizes of two adjacent cells should be set as closely as possible to avoid generating a big reflection. A structure of taper mesh whose cell size (c) varies gradually along a direction, such as expanding grid [8] is, in fact, a kind of MN.

B. MN Characteristics

A structure composed of cascade mesh sections with different cell sizes is called an MN. It has two types (Fig. 2). Fig. 2(a) shows the case in which the input mesh is different from the load mesh ($Z_0 \neq Z_\ell$). It looks like the traditional impedance transformer to match the mesh with a different MWI. Fig. 2(b) corresponds to the case in which $Z_0 = Z_\ell$. It is a kind of mesh structure inserted between two of the same meshes.

The network matrix of any MN can be expressed as

$$\begin{aligned}[A]_N &= \begin{bmatrix} A_{11} & A_{12} \\ A_{21} & A_{22} \end{bmatrix} \\ &= \begin{bmatrix} \cos\theta_1 & jZ_1\sin\theta_1 \\ \dfrac{j\sin\theta_1}{Z_1} & \cos\theta_1 \end{bmatrix} \\ &\quad \cdot \begin{bmatrix} \cos\theta_2 & jZ_2\sin\theta_2 \\ \dfrac{j\sin\theta_2}{Z_2} & \cos\theta_2 \end{bmatrix} \cdots \begin{bmatrix} \cos\theta_N & jZ_N\sin\theta_N \\ \dfrac{j\sin\theta_N}{Z_N} & \cos\theta_N \end{bmatrix} \\ &= [A]_{N-1} \begin{bmatrix} \cos\theta_N & jZ_N\sin\theta_N \\ \dfrac{j\sin\theta_N}{Z_N} & \cos\theta_N \end{bmatrix} \end{aligned} \tag{3}$$

where

$$\theta_i = \beta_i l_i, \qquad i = 1, 2, 3, \ldots. \tag{4}$$

Thus, the input impedance and total reflection coefficient of the MN are written, respectively, as

$$Z_m in = \frac{A_{11}\cdot Z_l + A_{12}}{A_{21}\cdot Z_l + A_{22}} \tag{5}$$

$$R = \frac{Z_m in - Z_0}{Z_m in + Z_0}. \tag{6}$$

Although the function of the network characteristic can be written easily by (3), it can only be used for strict analysis rather than synthesis of the MN. It is impossible to synthesize the MN with a traditional network method since the characteristic impedance of the transmission line of the microwave network is real, while Z_m and R of the MN, whose phases are frequency dependent, are generally complex.

Generally, the reflection between two adjacent mesh sections ($R_i, i = 1, 2, 3, \ldots, N$) is small, thus, some special characteristics may be obtained in an approximate way. It also presents an idea to synthesize these MNs.

When R_i is small, the total reflection coefficient of the MN can be rewritten as

$$\begin{aligned} R &\approx R_1 + R_2 e^{-j2\theta} + R_3 e^{-j4\theta} + \cdots + R_{N+1} e^{-j2N\theta} \\ &= \sum_{i=1}^{N+1} R_i e^{-j2(i-1)\theta}. \end{aligned} \tag{7}$$

From (5) and (6), we can see that the characteristics of the MN are mainly decided by the MWI (in fact, the cell-size factors c_i and the length of each section). For simplicity, the length of each section is set equal. The values of c_i are regularly changed. Suppose that c_i has a relation with the sections of the network

$$c_i = F(i), \qquad i = 1, 2, 3 \ldots, N \tag{8}$$

where N is the number of sections. The corresponding characteristic of the MN, such as a low-pass filter or an impedance transformer, can be reached by proper selection of F.

C. Match of Mesh Wave [$c_0 \neq c_{N+1}$, Fig. 2(a)]

1) Linear and Uniform Distribution of c_i: Suppose $c_0 < c_{n+1}$ (the case is similar if $c_0 > c_{n+1}$) and c_i distributes uniformly and varies linearly [see Fig. 3(a)], then

$$\begin{aligned} c_i &= c_0 + i\cdot\frac{(c_{N+1} - c_0)}{N+1} \\ &= c_0 + i\cdot\frac{\Delta c}{N+1}, \qquad i = 1, 2, 3 \ldots, N; \quad \Delta c = c_{N+1} - c_0. \end{aligned} \tag{9}$$

Since the magnitude of all R_i ($i = 1, 2, 3, \ldots$) is equal, (7) can be approximately rewritten as

$$R \approx |R'| \sum_{i=1}^{N+1} {}_i e^{-j2(i-1)\theta} = jtg\frac{k\cdot\Delta\cdot\Delta c}{4(N+1)} \cdot \sum_{i=1}^{N+1} {}_i e^{-j2(i-1)\theta}. \tag{10}$$

When the reflecting coefficient is at the minimal value for an MN with N sections, the following relation is satisfied:

$$\begin{aligned} 2(i-1)\theta &= \frac{2m\pi}{N+1}(i-1), \qquad i = 1, 2, 3 \ldots, N; \\ & m = 0, 1, 2, 3, \ldots. \end{aligned} \tag{11}$$

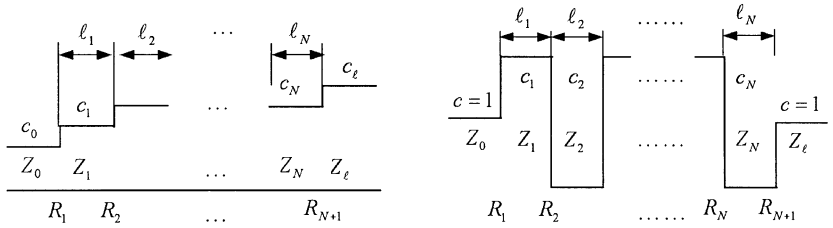

Fig. 2. Equivalent configuration of the transmission line for multisection stepped meshes. (a) $Z_0 \neq Z_\ell$. (b) $Z_0 = Z_\ell$.

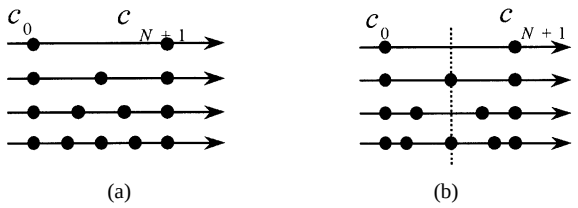

Fig. 3. Cell size changes linearly. (a) Uniform distribution. (b) Nonuniform distribution.

Namely,

$$\theta = \frac{m\pi}{N+1}, \qquad m = 0, 1, 2, 3, \ldots. \tag{12}$$

The corresponding frequency is

$$f = \frac{m}{2(N+1)\cdot\sqrt{\mu\varepsilon}\cdot l}, \qquad m = 0, 1, 2, 3, \ldots. \tag{13}$$

The frequency of the maximum point appears approximately in the middle of frequency of two minimal values

$$f = \frac{2m+1}{4(N+1)\cdot\sqrt{\mu\varepsilon}\cdot l}, \qquad m = 0, 1, 2, 3, \ldots. \tag{14}$$

From (10), (13), and (14), the magnitude of extreme value can be computed.

From the above analysis, we know that when the cell-size factors change linearly and uniformly, the reflection characteristic of MN with N sections is similar to the Chebyshev impedance transformer of the traditional microwave network as follows.

1) The extreme points of the reflecting coefficient within the matching band are periodical.
2) The extreme point of the MN with more sections has shorter period and smaller magnitude.
3) The more the sections of the MN, the wider the matching frequency band.
4) The numbers of the extreme value points within the effective frequency band is equal to the numbers of sections.

In addition, the shorter the length of each section, the wider the matching band. Also, the extreme values increase with the frequency.

Fig. 4 shows the reflecting characteristics of the MN ($\Delta =$ 1 cm, $l = 10$ cm, $c_0 = 1.0$, $c_{N+1} = 3.0$) when N equals 0, 1, and 2, respectively. The cell-size factors changes linearly and uniformly. Results from FDTD computation are also given. Two kinds of values are in agreement with each other. The shape of the curves is consistent with the above analysis. In addition, for a certain N, the maximum values of the ripple within the effective

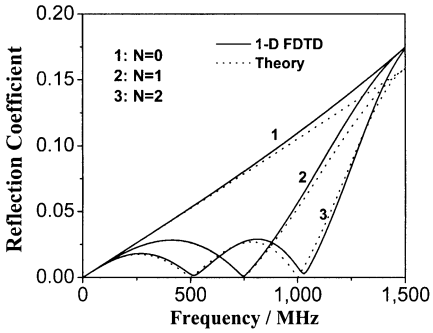

Fig. 4. Comparison of reflection characteristics of the MN when $N = 0, 1, 2$.

band are not equal. They increase with the frequency because the tangent function increases in a period, which is different from the traditional Chebyshev impedance transformer.

2) Linear and Nonuniform Distribution of c_i: By the same method, when c_i is

$$c_i = \left(c_0 - \frac{\Delta c}{2N}\right) + i\cdot\frac{\Delta c}{N}, \qquad i = 1, 2, 3, \ldots, N,\ N > 1. \tag{15}$$

A quasi-flat characteristic of an impedance transformer of the MN is obtained. The reflecting characteristics of the MN are compared in Fig. 5. We found that when the cell-size factor changes nonuniformly, the characteristics of the MN with N sections are similar to those of the MN with $N-1$ sections when cell-size factor changes uniformly, and it has flatter response in the useful frequency band.

Note that the so-called maxim flat impedance characteristic here is different from its original meaning. It comes from the above analysis.

D. Mesh Low-Pass Filter ($c_0 = c_{N+1}$)

For the MN when $c_0 = c_{N+1}$ [see Fig. 2(b)], using the character of MWR $jtg(-\Delta c) = -jtg((\Delta c))$ and symmetrically choosing the cell-size factor, a characteristic of a mesh low-pass filter can be obtained. It will be realized below.

The characteristics of the MN vary with $c_i = F(i)$ $(i = 1, 2, 3, \ldots, N)$. Thus, when the cell-size factors are selected properly, all kinds of characteristics of the MN can be achieved.

In addition, a similar analysis of a rectangular waveguide can find similar characteristics of the MN by means of MWI of the rectangular waveguide [9].

III. Synthesis and Realization

Analysis of the MN is different from that of a general microwave network. Its synthesis and realization are also different.

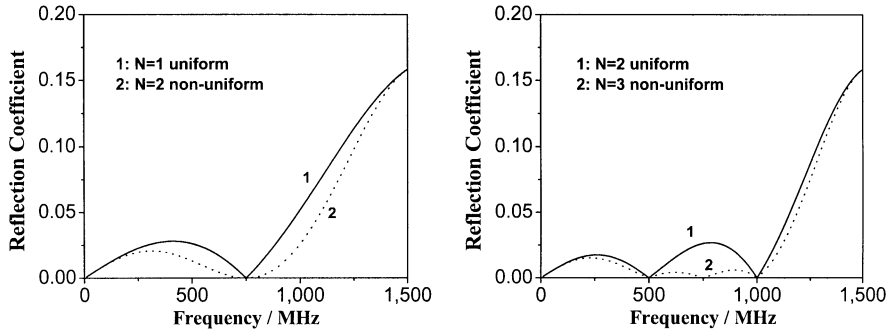

Fig. 5. Comparisons of the characteristic of an MN when the cell-size factors changes uniformly and nonuniformly, respectively, where $\Delta = 1$ cm, $\ell = 10$ cm, $c_0 = 1.0$, and $c_{N+1} = 3.0$.

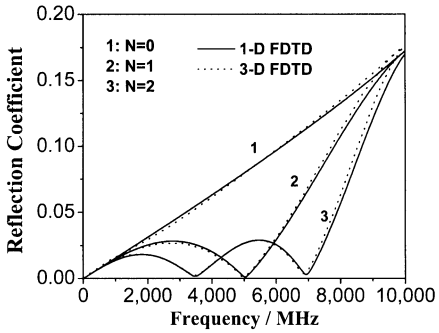

Fig. 6. Reflection coefficient of mesh impedance match in a microstrip.

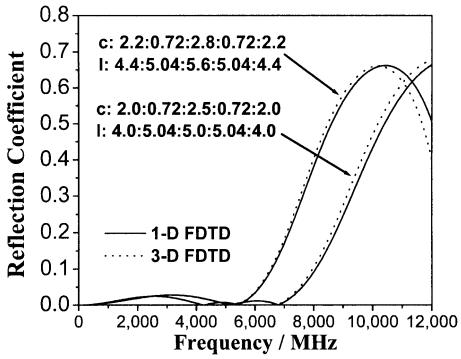

Fig. 7. Reflection coefficient of mesh-filter characteristics in a microstrip.

The idea for synthesis and realization can be obtained by analysis. For example, when the cell-size factor varies linearly, the synthesizing approaches are as follows.

The width of the passband can be obtained from (12) and (13) when the cell-size Δ and length ℓ of the sections are known and vice versa as follows.

1) The number of sections of the MN is decided by the cutoff frequency and cell size by (13).
2) When Δ, ℓ, and N are known, the maximum magnitude of the reflection within the passband is computed with (6) and (13).
3) The cell-size factor of the section can be decided by $c_i = F(i)$, which is used in FDTD computation.
4) The MWI used in theory computation is derived from (2) and (3).

The above discussion on the MN is for a 1-D TEM mode. It is, in practice, more useful for some three-dimensional (3-D) structure, e.g., a microstrip with a quasi-TEM mode. It has the same MN characteristics along the direction of propagation. Fig. 6 shows the characteristic of three kinds of impedance transformers with 1–3 sections, respectively. The impedance ratio between input and output is 3.0 in the center frequency. It is obvious that the characteristic is largely dependent on the number of sections. For the same impedance ratio, the more sections there are, the sharper the rising curve in the stopband and the wider the low-pass bandwidth. Comparing the curves in Fig. 6 with those in Fig. 3, we can see that the results of the 3-D case are also in agreement with those of the 1-D case.

Fig. 7 shows the characteristic of two mesh low-pass filters ($Z = Z_0$) of a microstrip line. The thickness of the substrate is 2 mm, the width of metal strip is 4 mm, $\varepsilon_r = 2.2$, and basic cell size is $\Delta = 1$ mm. Both MNs consist of five sections along the strip direction. It is shown that, for an MN with the same sections, the section has more cells, the reflection curves rise sharper in the stopband, and the passband is narrower. The computation results are also compared with those of 1-D simulation. They are in good agreement with each other, especially when frequency is low.

An exciting source for all FDTD simulations is the Gauss pulse. Any reflection ($R > 0.01$) from source and load ends will disturb the passband characteristic since the reflection of an MN is usually small. Thus, a good absorbing boundary is necessary.

It is usually difficult to divide sections at specific equal lengths since different sections have different cell sizes. Fortunately, the MWI's phase variation with frequency is approximately linear. By means of choosing cell-size factors c_i, the length of each section ℓ_i, and number of sections N_m, some network characteristics can be approximately obtained, which is useful in the application of the MN.

IV. Application

The mesh impedance transformer and the mesh low-pass filter are used to match or suppress the reflecting waves brought about by the nonuniformity of meshes. It enjoys advantages of saving memory and improving the computation efficiency of a nonuniform mesh. Application of these characteristics is demonstrated by the following three examples.

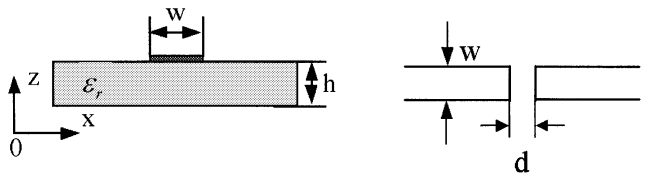

Fig. 8. Circuit structure of microstrip-gap capacitance.

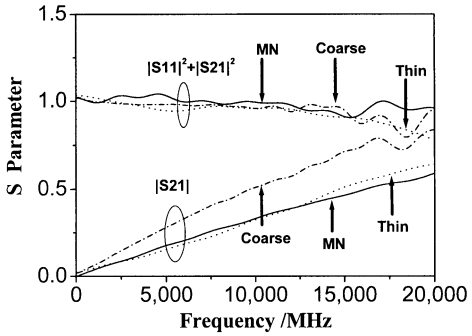

Fig. 9. S-parameters comparison of gap capacitance between the MN and uniform mesh.

A. Microstrip-Gap Capacitor

The size of the microstrip gap is usually small, but the field around it changes very sharply. The coarse cells are unable to describe it accurately, while the fineness cells cost memory. However, with the method presented in this paper, the problem can be solved with nonuniform mesh (i.e., MN) and the reflection can also be computed. The structure of the microstrip-gap capacitance is shown in Fig. 8, where $\varepsilon_r = 9$, $h = 1.2$ mm, $w = 1.2$ mm, and $d = 0.6$ mm.

In Fig. 9, the S-parameters of which no section of the MN is inserted, are compared with those in which one or two sections are inserted at the position before and behind the gap. The difference of $S21$ is not distinct. However, for the sum of $|S11|^2$ and $|S12|^2$ (Fig. 9), the useful frequency band without an MN is very narrow (with only 7 GHz), while the bandwidth of inserting one MN section is up to approximately 10 GHz. The results of inserting two sections are very close to those of the uniform thin mesh. The more MN sections are properly inserted, the better the match of the mesh wave, which is consistent with the analysis of Section III. It is obvious that using the MN requires less storage than using a thin mesh at a whole computation space and has a higher precision than using a coarse mesh.

According to the analysis of this paper, the resultant effect of the above MN in FDTD simulation can also be computed by (10) and (11). The curve of it is shown in Fig. 10. Setting the reference where the reflection is equal to 0.03 (approximately -30 dB), an interesting result is seen, i.e., the frequency character of the curves in Fig. 11 corresponds to those in Fig. 10, which verifies the results of Fig. 10 from another view.

B. Parallel-Coupling Filter

Characteristics of a parallel-coupling structure is sensitive to the coupling length and gap. Thus, in FDTD analysis, selecting a good mesh model is crucial. The coupling length and gap should be considered carefully. This example shows that a proper MN can save the storage without losing computation precision.

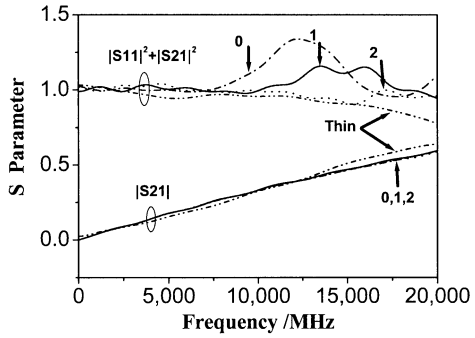

Fig. 10. Comparison of computation results of the MN with different sections.

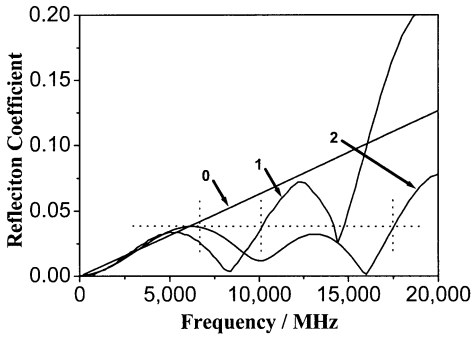

Fig. 11. Reflection characteristics of the MN with different sections.

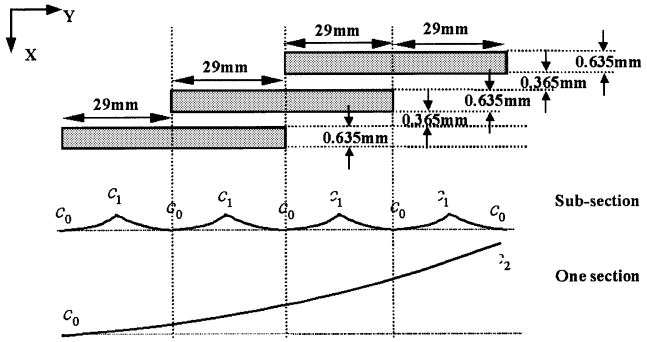

Fig. 12. Structure of a parallel-coupling filter where the thickness of substrate $h = 0.625$ mm: $\varepsilon_r = 9.9$.

The structure in Fig. 12 is very long in the propagation direction. Using a uniform mesh would cost storage. Thus, an MN is used. It is found that, for the MN whose cell-size factor varies exponentially (expanding girds), not only the reflection within the useful band is very small, but also the cost of storage remarkably decreases.

If using one section with a varying cell-size factor from input to output (shown in Fig. 12), the symmetry of the structure will be destroyed. Also. it is difficult for each section of the filter to occupy integral cells. In addition, the ratio of the sizes of the maximum cell at the output end and the minimal cell at the input end is large, which will make the useful frequency narrow since the cell size should usually be less than 1/10 of the shortest wavelength in order to decrease the mesh dispersion. Thus, a subsection meshing method is used (see Fig. 12). Also, the meshing result is compared in Table I. Each section of the filter has two subsections. The cell-size factors at two ends of the sections and at the middle of the sections are equal, respectively. The sizes at the ends are smaller than those at the middle position. They exponentially rise or fall, respectively.

TABLE I
COMPARISON OF DIFFERENT MESHING METHODS

Meshing method	Minimal cell size (mm)	Maximum cell size (mm)	Ratio of cell size	Total length (mm)	Total cells	Cells saved
Uniform	0.3625	0.3625	1.0000	29×4 (116)	320	/
Subsection	0.3625	0.6275	1.7310	15.0014×8 (116.00112)	30×8 (240)	80

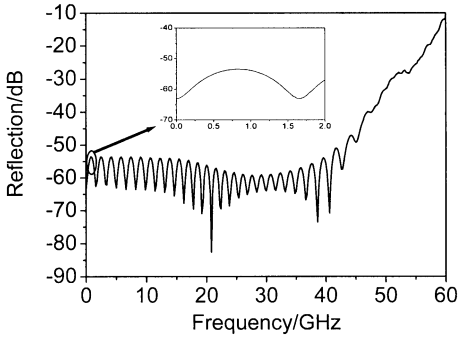

Fig. 13. Reflection characteristic of a subsection MN.

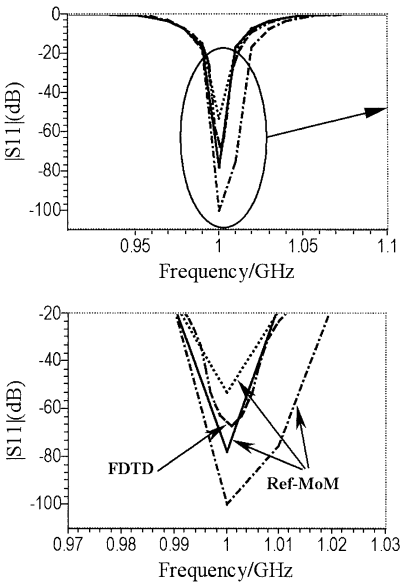

Fig. 14. Reflection characteristic of a parallel-coupling filter.

Suppose the cell size of a cell i is $c_i\Delta$, c_i is the cell-size factor varying exponentially, namely, $c_i/c_{i-1} = \alpha$. Table I makes a comparison between the meshing methods of the subsection and uniform. Set $\Delta = 0.3625$ mm and $a = 1.0191$ to ensure a whole-number division of each section. In Table I, it is seen that using the meshing method of a subsection may not only save 25% storage, but may also model the structure appropriately. The cell size in the X-direction is 0.1825 mm at the coupling gap and 0.216 67 mm at the metal strip.

An evaluation of the reflective effect of this MN for the filter characteristics can be done via the method of this paper. The result is given in Fig. 13. Reflection from a nonuniformed mesh is below -50 dB in 0∼43 GHz and -54 dB in 0∼2 GHz (specific band of [11]).

The resonate frequency of the reflection characteristic of the filter is shown in Fig. 14, which is in comparison with the results of [11]. Two kinds of values are in agreement with each other, which verifies that the method is reasonable.

C. Microstrip Slot-Line Transformer

The structure of the microstrip slot-line transformer is shown in Fig. 15, where $\varepsilon_r = 20$, $h = 3.175$ mm, $w_m = 1.5748$ mm, $L_m = 6.8834$ mm, $w_s = 2.0574$ mm, and $L_s = 6.8834$ mm. The structure is modeled by two meshing methods. One is a uniform mesh. The cell sizes in the three axes are $\Delta x = 0.4028$ mm, $\Delta y = 0.4064$ mm, and $\Delta z = 0.3969$ mm. Thus, there is a little difference between the mesh model and practical structure. Another method is using the MN, modeling the structure exactly in nonuniform mesh. The corresponding cell sizes are $\Delta z = 0.3969$ mm, $\Delta x_{Wm} = 0.3937$ mm, $\Delta x_{Ls} = 0.4064$ mm, $\Delta y_{Lm} = 0.3429$ mm, and $\Delta y_{Ws} = 0.3659$ mm (Fig. 15). There is only a little variation

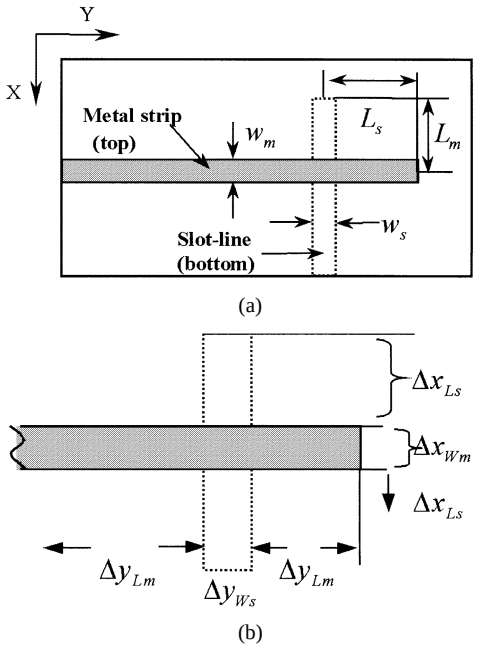

Fig. 15. Microstrip and slot-line transformer. (a) Structure. (b) Mesh model.

of the cell sizes in the direction of X and Y. The meshes at the position of metal strip (Δx_{Wm}, Δy_{Ws}) and slotline (Δx_{Ls}, Δy_{Lm}) are uniform, respectively.

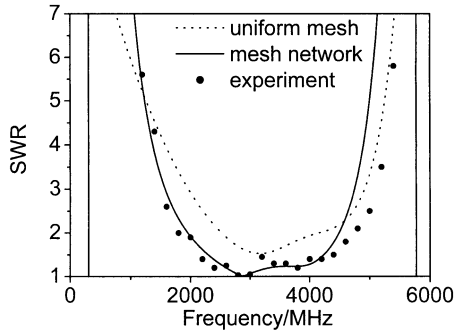

Fig. 16. SWR comparison of microstrip and slot-line transformer.

Fig. 16 gives input standing-wave ratios of the structure computed by the FDTD method in two mesh models. The experiment result [12] is also shown. In the effective frequency band (SWR < 2), results from the MN model are much more closer to the experiment than those from the uniform mesh. It indicates that the effect of the MN is less than L_s and L_m in this model. Also, the characteristic of the microstrip slot-line transformer is very sensitive to the change of their lengths. It also endorses strongly for the use of a nonuniform mesh (i.e., MN). The computation precision is remarkably improved by using a simple MN without modifying the FDTD computation program.

V. Conclusion

MN characteristics can be realized in FDTD numerical simulation by using the mesh sections with nonuniform meshes in cascade. Some MNs (such as a mesh impedance transformer and mesh low-pass filter) are found and presented. These MNs may be used in FDTD numerical simulation to match the mesh reflection wave of a nonuniform mesh, improve the mesh wave propagating condition, or purify the frequency spectrum at a specific passband. In many cases, an MN is built by a good selection of the section number and the cell number of each section, as well as the cell sizes, which cannot only save the memory storage, but also decrease the reflection from the nonuniformity of meshes in FDTD numerical simulation.

Principally, these MNs may be implemented in cases where a TEM or quasi-TEM wave propagates in the direction where the sizes of the meshes vary. It is easy to reach these network characteristics without the requirement of modifying the FDTD program.

References

[1] H. Sundqvist and G. Veronis, "A simple finite-difference grid with nonconstant intervals," *Tellus*, vol. 22, pp. 26–31, 1970.

[2] P. Thoma and T. Weiland, "A consistent sub-girding scheme for the finite different time domain method," *Int. J. Numer. Modeling*, vol. 9, pp. 359–374, 1996.

[3] S. Kapoor, "Sub-cellular technique for the finite difference time domain method," *IEEE Trans. Microwave Theory Tech.*, vol. 45, pp. 673–677, May 1997.

[4] E. A. Navarro, N. T. Sangary, and J. Litva, "Some considerations on the accuracy of the nonuniform FDTD method and its application to waveguide analysis when combine with the perfectly matched layer technique," *IEEE Trans. Microwave Theory Tech.*, vol. 44, pp. 1115–1124, July 1996.

[5] K. M. Krishnaiah and C. J. Railton, "A stable sub-girding algorithm and its application to eigenvalue problems," *IEEE Trans. Microwave Theory Tech.*, vol. 47, pp. 620–628, May 1999.

[6] W. H. Yu and R. Mittra, "A new sub-girding method for the finite-difference time-domain (FDTD) algorithm," *Microwave Opt. Technol. Lett.*, vol. 21, pp. 330–333, June 1999.

[7] ——, "A technique for improving the accuracy of the nonuniform finite-difference time-domain algorithm," *IEEE Trans. Microwave Theory Tech.*, vol. 47, pp. 353–356, Mar. 1999.

[8] B. Q. Gao and O. P. Gandhi, "A expanding-grid algorithm for the finite difference time domain method," *IEEE Trans. Electromagn. Compat.*, vol. 34, pp. 277–283, Aug. 1992.

[9] B. Q. Gao, "Mesh wave impedance concept in FDTD technique," *Electron. Lett.*, vol. 33, pp. 1610–1611, Sept. 1997.

[10] R. N. Ghose, *Microwave Circuit Theory and Analysis*. New York: McGraw-Hill, 1963.

[11] S. Ooms and A. De Zutter, "A new iterative diakoptics-based multilevel moments method for planar circuits," *IEEE Trans. Microwave Theory Tech.*, vol. 46, pp. 280–291, Mar. 1998.

[12] Y. M. M. Antar, A. K. Bhattcharyya, and A. Ittipiboon, "Microstripline–slotline transition analysis using the spectral domain technique," *IEEE Trans. Microwave Theory Tech.*, vol. 40, pp. 548–554, Mar. 1992.

[13] G. Mur, "Absorbing boundary condition for the finite-difference approximation of the time-domain electromagnetic-field equations," *IEEE Trans. Electromagn. Compat.*, vol. EMC-23, pp. 377–382, Apr. 1981.

[14] J. Berenger, "A perfectly matched layer for the absorption of electromagnetic waves," *J. Comput. Phys.*, pp. 185–200, 1994.

[15] C. E. Reuter, R. M. Joseph, E. T. Thiele, D. S. Katz, and A. Taflove, "Ultra wide band absorbing boundary condition for termination of waveguide structures in FD-TD simulations," *IEEE Microwave Guided Wave Lett.*, vol. 4, pp. 344–346, Oct. 1994.

[16] D. S. Katz, T. Thiele, and A. Taflove, "Validation and extension to three dimension of the Berenger PML absorbing boundary condition for FD-TD meshes," *IEEE Microwave Guided Wave Lett.*, vol. 4, pp. 268–270, Aug. 1994.

[17] W. Heinrich, K. Beilenhoff, P. Mezzanotte, and L. Roselli, "Optimum mesh grading for finite-difference method," *IEEE Trans. Microwave Theory Tech.*, vol. 44, pp. 1569–1574, Sept. 1996.

Yan Zhang received the B.E.E. degree in electromagnetic field and microwave technology from Xidian University, Xi'an, China, in 1992, and the Ph.D. degree in electronic engineering from the Beijing Institute of Technology, Beijing, China, in 2001.

From 1992 to 1996, she was with the Xi'an Research Institute of Electronic Engineering. She is currently a Post-Doctoral Fellow with the Shanghai Bell Ltd. Company, Shanghai, China, where she currently develops an RF and digital IF system of the base-station of third-generation (3G) mobile communication. Her research interests are computational electromagnetics and microwave integrated circuits.

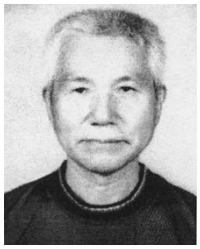

Ben-Qing Gao (M'95–SM'96) was born in Anhui Province, China. He received the Electronic Engineering degree from the Beijing Institute of Technology, Beijing, China, in 1959.

He then joined the faculty of the Beijing Institute of Technology. He was an Associate Professor in 1986. From January 1989 to September 1989, he was a Visiting Scholar with the Bioelectromagnetic Research Laboratory, University of Washington, Seattle. From October 1989 to September 1991, he was a Research Associate with the Electrical Engineering Department, University of Utah, Salt Lake City. He is currently a Professor and Ph.D. Supervisor with the Electronic Engineering Department, Beijing Institute of Technology. He has served on several Editorial Boards as an editor. His research interests include computational electromagnetics, microwave and millimeter-wave techniques, antennas and electromagnetic compatibility, etc. He has authored or coauthored four books and over 70 papers in journals.

Prof. Gao is a Fellow of the Chinese Institute of Electronics. He has served on various program committees as chair or co-chair for several international conferences.

Wu Ren received the B.E.E. degree in electromagnetic field and microwave technology from the Beijing Institute of Technology, Beijing, China, in 1998, and is currently working toward the Ph.D. degree in electromagnetic field and microwave technology at the Beijing Institute of Technology.

His current research interests are computational electromagnetics, microwave and millimeter-wave techniques, electromagnetic compatibility, and optoelectronics.

Zheng-Hui Xue received the B.E.E. and M.S. degrees in electromagnetic field and microwave technology from the Beijing Institute of Technology, Beijing, China, in 1992 and 1995, respectively.

He is currently an Associate Professor with the Electronic Engineering Department, Beijing Institute of Technology. He has authored or coauthored over 20 papers. His current research interests are computational electromagnetics, microwave integrated circuits, and electromagnetic compatibility.

Wei-Ming Li received the B.S. degree from the Jiangxi Normal College, Nanchang, China, in 1988, and the Ph.D. degree from the Beijing Institute of Technology, Beijing, China, in 2001.

From 1993 to 1997, he was a Marketing Engineer with the Jiangling Automobile Corporation, Nanchang, China. He is currently an Associate Professor with the Electronic Engineering Department, Beijing Institute of Technology. His current research interests include computational electromagnetic and RCS of complex objects.